2013 IEEE/RSJ International Conference on
Intelligent Robots and Systems (IROS)
November 3-7, 2013. Tokyo, Japan

Human Like Learning Algorithm for Simultaneous Force Control and Haptic Identification

Chenguang Yang, Zhijun Li and Etienne Burdet

Abstract— **This paper develops a learning control algorithm adapting the reference point and force to interact with an object of unknown geometry and elasticity. The controller is inspired by neuroscience studies that investigated the neural mechanisms when human adapt to virtual objects of different properties. The learning control algorithm estimates the shape and stiffness of the given object while maintaining a specified contact force with the environment. Simulations demonstrate the efficiency of the algorithm to identify the geometry and impedance of an unknown object without requiring force sensing. These properties are attractive for robotic haptic exploration with little demand on the sensing.**

I. Introduction

Human beings are able to estimate the shape and texture of arbitrary objects using haptic exploration with the hand (Fig. 1). In contrast, robotic control schemes are designed for specific tasks. Although many tasks such as polishing or carving require to explore the contact surface, only few works have been devoted to haptic exploration. Surface exploration geometry is performed using only haptics [1], [2], [3], [4], [5] or additionally aided by vision [6], [7]. These techniques aim either to reconstruct an object 3D geometry[8], [9], [10] or to determine its texture [11] using dedicated tactile or force sensors [12], [13] and applying little contact force. However, tasks requiring a mechanical interaction such as polishing or carving require the application of relatively large force on the surface, usually involving penetration of the object's surface, and vision is of little help to determine the irregularities and variations of the surface. In this context, we introduce here a versatile controller that is able to maintain a significant force on the object, and to detect an object's properties like stiffness and shape/boundary without requiring any force sensor.

Three main approaches have been developed to control the interaction of robots with the environment:

- The *hybrid force/position control* process [14], [15] is divided between contact and noncontact phases, with transitions requiring accurate model of the contact surface, while inaccurate detection of position or timing will lead to jerky transitions.
- *Impedance/admittance control* [16] does not attempt to track desired motion or force but rather to regulate the dynamics between them by using a target impedance model. However, in the case of a large obstacle, the force against the surface will grow with the distance to the reference trajectory, which may damage the object or the robot.
- *Parallel force/position control* [17] was developed to avoid these problems, in which the force control loop is designed to prevail over the position control loop. However, this strategy still requires knowledge of the geometry of the surface on which the force has to be exerted.

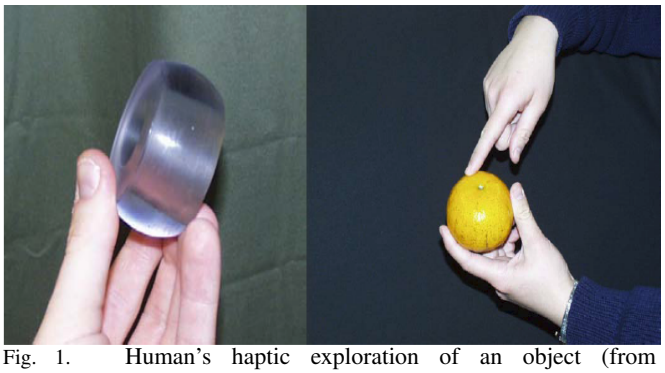

Fig. 1. Human's haptic exploration of an object (from http://lims.mech.northwestern.edu/projects/fingertip/index.html).

These conventional controllers can be used to perform well defined tasks in a known environment. For example, drilling may be achieved by impedance control with carefully tuned impedance parameters, and polishing of an object with known geometry may be achieved using hybrid control by controlling position tangential to the surface and force normal to it. However these strategies may fail when little a priori knowledge of the task or of the environment/external object is available.

In contrast, humans can interact with various kinds of objects or new dynamic environments even without using vision. This has motivated the study of how humans interact with a novel virtual force field generated by a robotic interface [18], [19], [20]. In a series of studies, e.g. [19], [21], we have shown that the human central nervous system (CNS) selectively adapts muscles activation to maintain the same stability margin in stable or unstable interactions as in free movements. The human CNS adapts endpoint force and

[1]School of Computing and Mathematics, University of Plymouth, UK. [2]Key Laboratory of Autonomous Sysems and Netowked Control, Ministry of Education, Guangzhou, 510640, China. [3] Department of Bioengineering, Imperial College of Science, Technology and Medicine, London, UK. Email: cyang@ieee.org; zli@ieee.org; e.burdet@imperial.ac.uk. This work was supported in part by the Marie Curie International Incoming Fellowship H2R Project (FP7-PEOPLE-2010-IIF-275078), by the Foundation of Key Laboratory of Autonomous Systems and Networked Control, Ministry of Education, China (ASNC1201), by the the Natural Science Foundation of China (61174045, 61111130208, 60935001), by the RS-NSFC International Exchange project (JP100992), by the International Science and Technology Cooperation Program of China (0102011DFA10950), by the UKIERI "A sensor-based training system for home rehabilitation" project, by the EU-FP7-PEOPLE-ITN CONTEST project, and by the Fundamental Research Funds for the Central Universities (2011ZZ0104).

mechanical impedance as has been described in [22], which gave rise to a novel robotic adaptive controller analysed and demonstrated in [23].

In a recent experiment [20] observed how human subjects differently adapt the control to interact with objects of different stiffnesses. The CNS compensates for the interaction force with a compliant object, but it adapts the reference trajectory to go around a stiff object and avoid excessive force. This trajectory adaptation has been modelled in [24], however the control scheme required force sensing (while many generic robot platforms are not equipped with force sensors), and feedforward force was not adapted.

In [25], we implemented reference adaptation without using force measurement and applied our algorithm to haptic surface detection. However, no mathematical analysis of this algorithm was provided in these papers. Furthermore, the algorithm focused on adaptation of the robot impedance along the motion and assumed an object elasticity. In the present paper, we develop an algorithm for the adaptation of force and trajectory that can control the interaction force and identify the environment geometry and elasticity in one degree of freedom, analyse it mathematically and demonstrate it in simulations.

II. Controller

Consider a non-redundant robot with n joint variables $q \in \mathbb{R}^n$ with $\mathbb{R}$ denoting the set of real numbers. The end effector of the robot moves in the 6 degree of freedom (DOFs) Cartesian space and its position is denoted by $x \in \mathbb{R}^6$. The forward kinematics is a mapping between q in joint space and x in Cartesian space, which can be described by a nonlinear function $x = \phi(q)$. Differentiating $x = \phi(q)$ with respect to time yields

$$\dot{x} = J(q)\dot{q}\,, \quad \ddot{x} = J(q)\ddot{q} + \dot{J}(q)\dot{q}\,, \tag{1}$$

where $J(q) = \left(\frac{\partial \phi_i}{\partial q_j}(q)\right) \in \mathbb{R}^{m\times n}$ is the Jacobian matrix. We assume the robot dynamics can be described by the rigid body dynamics model as follows:

$$M(q)\ddot{q} + N(q,\dot{q}) = \tau - J^T(q) f_I \tag{2}$$

where $M(q)$ is the (symmetric, positive definite) mass matrix, $N(q,\dot{q})$ is the nonlinear term representing the joint torque vector due to the centrifugal, Coriolis, gravitational and friction forces, τ is the vector of joint torques, and f_I is the force applied by the end effector on the environment.

Since the task of haptic exploration is defined in the operational Cartesian space, we transfer the above dynamics (2) to the operational Cartesian space. To do so, by considering the kinematics (1) and dynamics (2), we obtain the manipulator dynamics in the Cartesian space as

$$M_x(q)\,\ddot{x} + N_x(q,\dot{q}) = f - f_I \tag{3}$$

where $M_x(q) = J^{-T}(q)M(q)J^{-1}(q)$ is also symmetric and positive definite, $N_x(q,\dot{q}) = J^{-T}(q)(N(q,\dot{q}) - M(q)J^{-1}(q)\dot{J}(q)\dot{q})$, and $f = J^{-T}(q)\tau$, which is the force (in fact, the wrench) applied on the end effector in the Cartesian space corresponding to the joint torque τ. As the motor torque at each joint can be obtained by $\tau = J^T f$, in the rest of the paper we simply regard f as control input.

To drive the robot end effector on a given reference point (pose, i.e. position and orientation) $x_r \in \mathbb{R}^6$, a simple controller

$$f = N_x - C_r\,\dot{x} - K_r(x - x_r) \tag{4}$$

could be employed with positive diagonal matrices C_r and K_r as reference damping and reference stiffness, respectively, which guarantees that $x \to x_r$. To maintain a contact force between robot end effector and the object, we add a feedforward force term in the above controller:

$$f = N_x - C_r\,\dot{x} - K_r(x - x_r) + f_r \tag{5}$$

where f_r is the reference force to be applied on the object by the end effector. Substitution of controller (5) into robot dynamics (3) yields

$$M_x(q)\,\ddot{x} + C_r\,\dot{x} + K_r(x - x_r) = f_r - f_I\,. \tag{6}$$

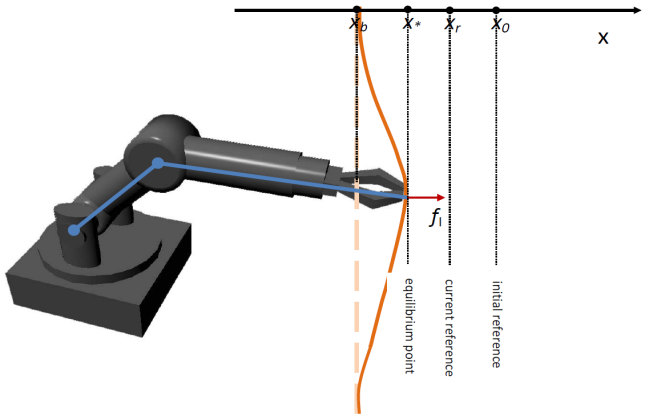

Fig. 2. Robot end effector's interaction with and exploration of an unknown object.

III. Adaptation and Learning

To simplify the exposition, we assume below that the robot end effector moves and interacts with objects only in the x direction of the Cartesian space as illustrated in Fig. 2. However the algorithms can be developed in the same way in the three axes x, y and z. Assume that the values of $C_r \in \mathbb{R}$, $K_r \in \mathbb{R}$ and initial reference point $x_t \in \mathbb{R}$ are well chosen such that the end effector smoothly approaches and then presses the unknown object without breaking it. Damping C_r is chosen to avoid excessive speed and to bounce back, and stiffness K_r to generate a compliant driving force together with reference x_r which is initially equals to x_t and inside the object boundary. We denote the position at which the robot end effector first touches the object in a trial as x_b and the object's stiffness as K_o, then the elastic response to robot end effector's pressure is

$$f_I = K_o(x - x_b) \tag{7}$$

when the end effect is in contact with the object. Combining (6) and (7) yields the closed-loop dynamics during contact:

$$M_x(q)\,\ddot{x} + C_r\,\dot{x} + K_r(x - x_r) + K_o(x - x_b) = f_r \qquad (8)$$

Considering that $M_x(q)$, C_r, K_r and K_o are all positive, the dynamics in the above equation is stable.

A. Adaptation of reference position and force

We consider for each trial a finite time T, which is sufficiently large such that at instant T the robot end effect has reached the equilibrium point x_* interacting with the object, and at the equilibrium point we should have

$$K_o(x_* - x_b) = -K_r(x_* - x_r) + f_r \qquad (9)$$

Denoting $e = x_* - x_r$, we propose the following adaptation law of reference point x_r from trial i to $i+1$:

$$\begin{aligned} x_r^1 &= x_t\,, \quad i = 1, 2, 3, \ldots && (10)\\ x_r^{i+1} &= x_r^i + \alpha^i e^i + (1-\alpha^i)(x_t - x_r^i) \;\text{ if }\; e^i \le 0 \\ x_r^{i+1} &= x_r^i + (1-\alpha^i)(x_t - x_r^i) \;\text{ otherwise}\,, && (11)\end{aligned}$$

where $0 < \alpha^i < 1$ is a compliance factor. The larger it is the more the reference point would change to be compliant to the object while the smaller it is the less the reference point would adapt and thus the robot appears to be less compliant and sticks to the last reference point. The human motor control experiment in [20] revealed that when human subjects interacting with a compliant/soft object, they use a compensatory response tending to reach the reference in free movement, while when the object is stiff they will modify the reference to follow the object's border. This observation inspires us to choose the compliance factor α^i in accordance to the estimation of the object stiffness as will be defined later in Equ.(20).

When e^i is larger than zero, in other words, the robot end effector is beyond the reference set point, either there is extra feedforward force or the object stiffness is reduced, e.g., the object has been removed or replaced with a softer object. In the former case, feedforward force is reduced as in Equ.(12) while in the latter case, x_r is adapted back to the original reference point, e.g., when the object is removed, the robot end effector should tend to restore back.

From (9) we see that the contact force at the equilibrium of ith trial is $f_I^i = -K_r e^i + f_r^i$. In order to maintain the contact force f_I unchanged, then the increase or decrease of f_r should be compensated by the decrease or increase of $K_r e$. This inspires the following adaptation law of feedforward force:

$$\begin{aligned} f_r^1 &= f_0\,, \quad i = 1, 2, 3, \ldots && (12)\\ f_r^{i+1} &= f_r^i + K_r(e^i - e^{i-1}) + \beta^i(f_0 - f_r^i) \;\text{ if }\; e^i \le 0 \\ f_r^{i+1} &= f_r^i + \beta^i(f_0 - f_r^i) \;\text{ otherwise}\,, && (13)\end{aligned}$$

where $0 < \beta^i < 1$ is a relaxation factor which tends to push f_r back to the value of f_0, the default contact force. When a human holds an object with high stiffness such as a glass, s/he has to carefully control the contact force in order to prevent dropping it, while when the object is elastic such that it is easier to hold s/he can relax the applied force. Therefore, we should set this relaxation factor such that the larger the objective stiffness is, the smaller it should be, as will be defined in (20).

B. Learning the object elasticity

In this section we derive algorithms to estimate the object's stiffness K_o and its border x_b. For convenience we set

$$\theta_1 \equiv \frac{K_r}{K_o}, \quad \theta_2 \equiv x_b\,. \qquad (14)$$

At the end of each trial, assuming that equilibrium has been rearched, we see from (9) that

$$\frac{x_*^i}{x_*^i - x_r^i} - \frac{\theta_2}{x_*^i - x_r} = \theta_1\left(\frac{f_r^i}{K_r(x_*^i - x_r^i)} - 1\right)$$

Let us set $s^i \equiv \frac{x_*^i}{x_*^i - x_r^i}$, $\phi_1^i \equiv \frac{f_r^i}{K_r(x_*^i - x_r^i)} - 1$ and $\phi_2^i \equiv \frac{1}{x_*^i - x_r^i}$ to simplify the presentation of the above equation as:

$$s^i = \theta_1\phi_1^i + \theta_2\phi_2^i \equiv \Theta^T\Phi^i \qquad (15)$$

with $\Theta \equiv (\theta_1, \theta_2)^T$ and $\Phi \equiv (\phi_1, \phi_2)^T$.

As Equ.(15) is linear in the parameters, an estimator such as gradient descent or the recursive least square method can be used to estimate θ_1 and θ_2. For fast convergence, we employ the following weighted least square (WLS) [26]:

$$\begin{aligned} \hat{\Theta}^{i+1} &= \hat{\Theta}^i + L^i(s^{i+1} - \hat{\Theta}^{iT}\Phi^i) \\ L^i &= \frac{P^i\Phi^i}{\omega^{i^{-1}} + \Phi^{i^T}P^i\Phi^i} \qquad (16)\\ P^{i+1} &= P^i - \frac{P^i\Phi^i\Phi^{iT}P^i}{\omega^{i^{-1}} + \Phi^{i^T}P^i\Phi^i} \\ i &= 1, 2, 3, \ldots \end{aligned}$$

where $\hat{\Theta}^i = (\hat{\theta}_1^i, \hat{\theta}_2^i)^T$ is the estimate of Θ. The estimates of K_o and x_b at the ith trial (denoted as $\hat{K}_o^i$ and $\hat{x}_b^i$) are thus

$$\hat{K}_o^i \equiv \frac{K_r}{\hat{\theta}_1^i}, \quad \hat{x}_b^i \equiv \hat{\theta}_2^i, \quad \text{if} \quad e^i \le 0\,. \qquad (17)$$

Mathematically, $\hat{\Theta}^0$, the initial estimate of Θ can be chosen arbitrarily, we take simply $\hat{K}_o^1 = \hat{K}_o^0 = \bar{K}_o$ and $\hat{x}_b = x_s$, where $\bar{K}_o$ is the largest possible object stiffness and x_s is the initial position of robot end effector. In haptic exploration without vision, one can conservatively assume that the object is hard and large before planning out motion in order to avoid excessive bouncing force or breaking it when touching it. When $e^i > 0$, we can assume that the object is removed or has been changed (if neither of these cases happens, but there just is extra feedforward force, then (12) will reduce the f_r such that e^i will be nonpositive again) so

$$\hat{K}_o^i \equiv \beta^i K_o^{i-1}, \quad \hat{x}_b^i \equiv \alpha^i\hat{x}_b^{i-1} + (1-\alpha^i)x_t \quad \text{if} \quad e^i > 0 \qquad (18)$$

The initial value of P in (16) can be simply chosen as $P^0 = I$ with I the identity matrix, and the weighting sequence ω^i is given by

$$\omega^i = \frac{1}{log^{1+\delta}(1 + \sum_0^i \|\Phi^i\|^2)} \qquad (19)$$

such that the convergence of $\hat{\Theta}^i$ is guaranteed even in the presence of a large amplitude random noise.

Using the estimate of K_o available, we can now turn to the problem of defining the values of compliance factor α_i and relaxation factor β_i in (10) and (12), respectively. We choose these factors as:

$$\alpha^i = \lambda \frac{\hat{K}_o}{\bar{K}_o}, \quad \beta^i = 1 - \alpha^i \tag{20}$$

with λ a constant to be specified by the user.

IV. Simulations

To verify the effectiveness of the proposed control algorithm, we carried out simulations (using the MATLAB/SIMULINK robotics toolbox of [27]). We simulated the interaction of one arm with an object, and the grasping of an object with two arms, with manipulators moving in the $x-y$ plane (Fig.3).

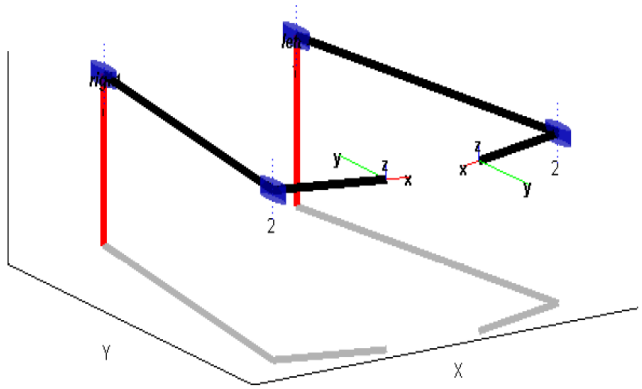

Fig. 3. Robot model in SIMULINK used in our simulations. Only the right arm is used for the first simulation.

Using the abbreviation $s_{12} = \sin(q_1+q_2)$, $c_{12} = \cos(q_1+q_2)$, $c_1 = \cos(q_1)$, $s_1 = \sin(q_1)$, $s_2 = \sin(q_2)$, and $c_2 = \cos(q_2)$, we specify the kinematics and dynamics of the robot as follows:

$$J(q) = \begin{bmatrix} -(l_1 s_1 + l_2 s_{12}) & -l_2 s_{12} \\ l_1 c_1 + l_2 c_{12} & l_2 c_{12} \end{bmatrix} \tag{21}$$

and

$$M(q) = \begin{bmatrix} M_{11} & M_{12} \\ M_{21} & M_{22} \end{bmatrix}, \; N(q,\dot{q}) = \begin{bmatrix} C_{11} & C_{12} \\ C_{21} & C_{22} \end{bmatrix} \tag{22}$$

where $M_{11} = m_1 l_{c1}^2 + m_2(l_1^2 + l_{c2}^2 + 2 l_1 l_{c2} c_2) + I_1 + I_2$, $M_{12} = M_{21} = m_2(l_{c2}^2 + l_1 l_{c2} c_2) + I_2$, $M_{22} = m_2 l_{c2}^2 + I_2$, $C_{11} = -m_2 l_1 l_{c2} s_2 \dot{q}_2$, $C_{12} = -m_2 l_1 l_{c2} s_2 (\dot{q}_1 + \dot{q}_2)$, $C_{21} = m_2 l_1 l_{c2} s_2 \dot{q}_1$, $C_{22} = 0$, where m_i, l_i, I_i, l_{ci}, $i = 1, 2$ represent the mass, length, inertia about the z-axis that comes out of the page passing through the center of mass, and the distance from the previous joint to the center of mass of link i, respectively. We set $m_1 = m_2 = 10.0kg$, $l_1 = l_2 = 1.0m$, $I_1 = I_2 = 0.83kgm^2$, $l_{c1} = l_{c2} = 0.5m$. Adaptive control is implemented on the x-axis with $C_r = 70Ns/m$ and $K_r = 20N/m$ while a position is maintained on the y-axis. The duration for each trial is set as $T = 30s$, the default feedforward force is set as $F_0 = 0N$ and the largest possible object stiffness as $\bar{K}_o = 500N/m$.

A. Unimanual control and identification

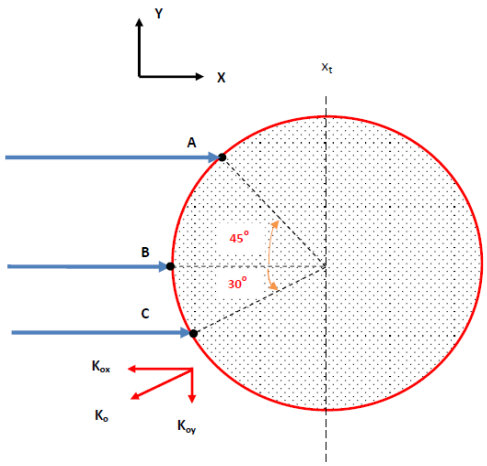

Fig. 4. Unimanual control and haptic identification.

The setup of unimanual control simulation experiment is shown in Fig.(4). The object is a disk with center $(1.5, 0)m$ and radius $0.5m$. The robot is position controlled to move along the y-axis at point A, then B and C. The stiffness of the circle object along normal direction is $100N/m$ and then the x-axis stiffness at A, B and C is $70.7107N/m$, $100N/m$, and $86.6025N/m$, respectively. The border point at A, B and C is $1.1464m$, $1.0m$ and $1.0670m$, respectively. At each of these three positions, the robot has 20 trials for exploration.

B. Bimanual control and identification

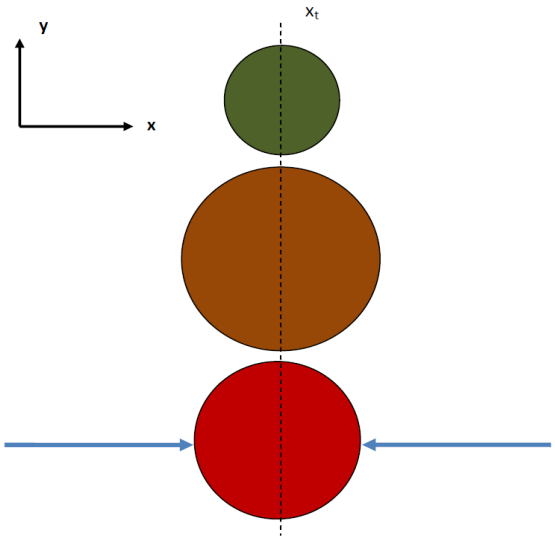

Fig. 5. Bimanual control and haptic identification.

The setup of the bimanual control simulation experiment is shown in Fig.5. The two robot arms are controlled to move along the x-axis, from outside to inside, while the three circular objects will be put in between the arms one by one in a sequence. When the object is in between the two arms, the center of the circle is at $(1.5, 0)m$, and the initial

reference point is set as $x_t = 0$. The radius and the stiffness of the three objects are $(0.5m, 200N/m)$, $(0.8m, 100N/m)$ and $(0.3m, 150N/m)$, respectively. The border point of these three objects are $1.0m$, $0.7m$ and $1.2m$, respectively.

The simulation results are shown in Fig.6 and Fig. 7. The first two panels in each figure show the identification of x_b and K_o and the last the contact force at the end of each trial, which is the force that the robot end effector applied on the object at the equilibrium. From Equ.(9), this force f_c can calculated as $f_c = f_r + K_r(x_r - x_*)$. For the unimanual experiment, the four stages for points A, B, C and empty objects are shown in lines of red circle, blue star, green circle and red star, respectively. For the bimanual experiment, the three stages correspond to identification of the three objects are shown in lines of red circle, blue star and green circle, respectively. We see that the estimated object stiffness K_o and geometric border point x_b match well with the true value, even in the presence of switch of robot end effector contact point and object. When the external object is removed, i.e., in stage 4 of case (i), the algorithm is able to identify zero object stiffness in the absence of interaction with the object.

V. Conclusion

This paper developed a biomimetic learning control algorithm for the interaction of a robot with objects of unknown geometry and mechanical properties. This adaptive algorithm can maintain a nearly constant contact force, while identifying the object geometry and stiffness during interaction. Interestingly, this is obtained without requiring measurement of the contact force (thus not requiring an expensive force sensor), by relying on a novel observer and on a good calibration of the robot force. Simple simulations of one degrees of freedom movements demonstrated the efficiency of this novel adaptive controller, while the extension to the multidimensional case and its implementation will be reported in our subsequent work. This controller shows similar adaptation as observed in humans adapting to unknown (virtual) objects [20] and may thus be used as a model of this adaptation.

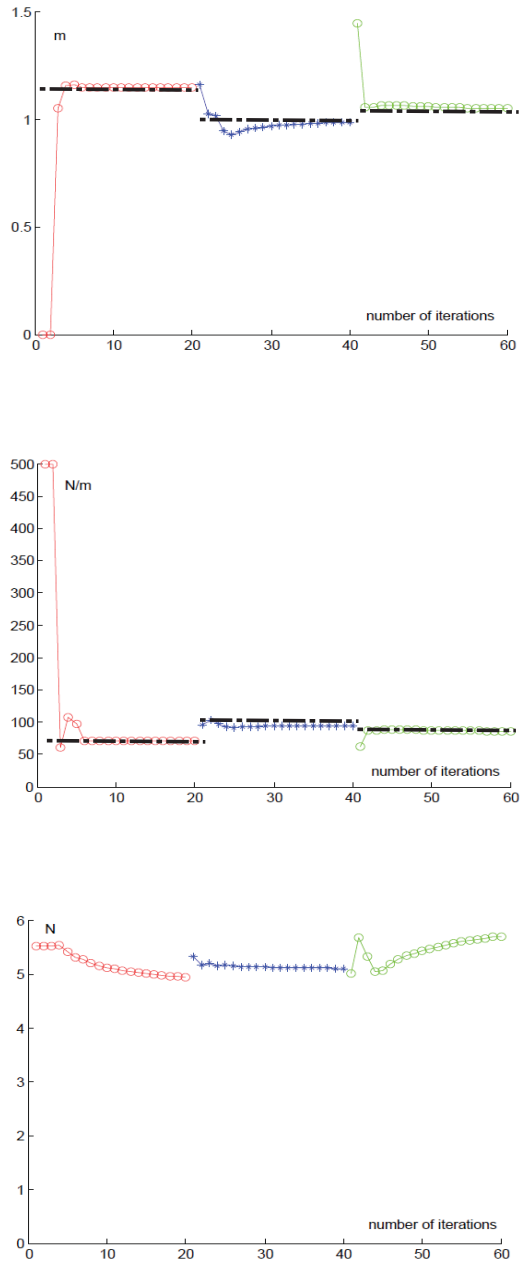

Fig. 6. Unimanual exploration of an object shown in Fig. 4; iterations 1-20 at point A; 21-40 at point B; 41-60 at point C. (a) Estimation of x_b (black dashed line for true values). (b) Estimation of K_o (black dashed line for true values). (c) Contact force.

References

[1] K. Pribadi, J. Bay, and H. Hemami, "Exploration and dynamic shape estimation by a robotic probe," *Systems, Man and Cybernetics, IEEE Transactions on*, vol. 19, no. 4, pp. 840–846, 1989.

[2] S. Sestili and A. Starita, "Learning objects by tactile perception," in *Engineering in Medicine and Biology Society, 1989. Images of the Twenty-First Century., Proceedings of the Annual International Conference of the IEEE Engineering in*, pp. 896–897, IEEE, 1989.

[3] P. Dario, M. Bergamasco, and A. Sabatini, "Sensing body structures by an advanced robot system," in *Robotics and Automation, 1988. Proceedings., 1988 IEEE International Conference on*, pp. 1758–1763, IEEE, 1988.

[4] S. A. Stansfield, "Haptic perception with an articulated, sensate robot hand," *Robotica*, vol. 10, no. 6, pp. 497–508, 1992.

[5] A. M. Okamura and M. R. Cutkosky, "Haptic exploration of fine surface features," in *Robotics and Automation, 1999. Proceedings. 1999 IEEE International Conference on*, vol. 4, pp. 2930–2936, IEEE, 1999.

[6] A. M. Okamura and M. Curkosky, "Feature-guided exploration with a robotic finger," in *Robotics and Automation, 2001. Proceedings 2001 ICRA. IEEE International Conference on*, vol. 1, pp. 589–596, IEEE, 2001.

[7] H. T. Tanaka, K. Kushihama, N. Ueda, and S.-i. Hirai, "A vision-based haptic exploration," in *Robotics and Automation, 2003. Proceedings. ICRA'03. IEEE International Conference on*, vol. 3, pp. 3441–3448, IEEE, 2003.

[8] A. Bierbaum, M. Rambow, T. Asfour, and R. Dillmann, "A potential field approach to dexterous tactile exploration of unknown objects," in *Humanoid Robots, 2008. Humanoids 2008. 8th IEEE-RAS International Conference on*, pp. 360–366, IEEE, 2008.

[9] F. Mazzini, D. Kettler, S. Dubowsky, and J. Guerrero, "Tactile robotic mapping of unknown surfaces: an application to oil well exploration," in *Robotic and Sensors Environments, 2009. ROSE 2009. IEEE International Workshop on*, pp. 80–85, IEEE, 2009.

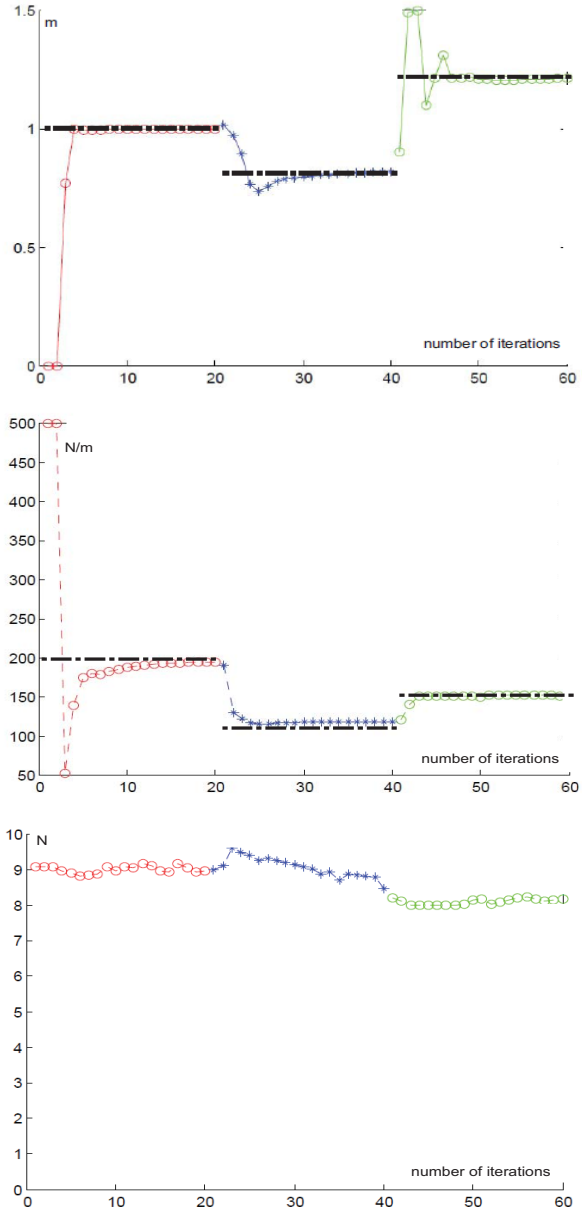

Fig. 7. Bimanual explorations of objects shown in Fig. 5, iterations 1-20 for the 1st object, 21-40 for the 2nd object, and 41-60 for the 3rd object. (a) Estimation of x_b (black dashed line for true values) . (b) Estimation of K_o (black dashed line for true values). (c) Contact force.

[10] D. R. Faria, R. Martins, J. Lobo, and J. Dias, "Probabilistic representation of 3d object shape by in-hand exploration," in *Proceedings of the 2010 IEEE/RSJ International Conference on Intelligent Robots and Systems, IROS*, vol. 10, 2010.

[11] W. Mayol-Cuevas, J. Juarez-Guerrero, and S. Munoz-Gutierrez, "A first approach to tactile texture recognition," in *Systems, Man, and Cybernetics, 1998. 1998 IEEE International Conference on*, vol. 5, pp. 4246–4250, IEEE, 1998.

[12] D. Kraft, A. Bierbaum, M. Kjaergaard, J. Ratkevicius, A. Kjaer-Nielsen, C. Ryberg, H. Petersen, T. Asfour, R. Dillmann, and N. Kruger, "Tactile object exploration using cursor navigation sensors," in *EuroHaptics conference, 2009 and Symposium on Haptic Interfaces for Virtual Environment and Teleoperator Systems. World Haptics 2009. Third Joint*, pp. 296–301, IEEE, 2009.

[13] P. A. Schmidt, E. Maël, and R. P. Würtz, "A sensor for dynamic tactile information with applications in human–robot interaction and object exploration," *Robotics and Autonomous Systems*, vol. 54, no. 12, pp. 1005–1014, 2006.

[14] M. D. Queiroz, J. Hu, D. Dawson, T. Burg, and S. Donepudi, "Adaptive position/force control of robot manipulators without velocity measurements: Theory and experimentation," *IEEE Transactions on Systems, Man and Cybernetics-Part B: Cybernetics*, vol. 27, no. 5, pp. 796–809, 1997.

[15] O. Khatib, "A unified approach for motion and force control of robot manipulators- The operational space formulation," *IEEE Journal of Robotics and Automation*, vol. 3, no. 1, pp. 43–53, 1987.

[16] N. Hogan, "Impedance control: an approach to manipulation-Part I: Theory; Part II: Implementation; Part III: Applications," *Transaction ASME J. Dynamic Systems, Measurement and Control*, vol. 107, no. 1, pp. 1–24, 1985.

[17] B. Siciliano, L. Sciavicco, L. Villani, and G. Oriolo, *Robotics: modelling, planning and control*. Springer, 2011.

[18] R. Shadmehr and F. A. Mussa-Ivaldi, "Adaptive representation of dynamics during learning of a motor task," *Journal of Neuroscience*, vol. 14, no. 5, pp. 3208–3224, 1994.

[19] E. Burdet, R. Osu, D. W. Franklin, T. E. Milner, and M. Kawato, "The central nervous system stabilizes unstable dynamics by learning optimal impedance," *Nature*, vol. 414, no. 6862, pp. 446–449, 2001.

[20] V. S. Chib, J. L. Patton, K. M. Lynch, and F. A. Mussa-Ivaldi, "Haptic identification of surfaces as fields of force," *Journal of Neurophysiology*, vol. 95, no. 2, pp. 1068–1077, 2006.

[21] D. W. Franklin, G. Liaw, T. E. Milner, R. Osu, E. Burdet, and M. Kawato, "Endpoint stiffness of the arm is directionally tuned to instability in the environment," *Journal of Neuroscience*, vol. 27, no. 29, pp. 7705–7716, 2007.

[22] K. P. Tee, D. W. Franklin, M. Kawato, T. E. Milner, and E. Burdet, "Concurrent adaptation of force and impedance in the redundant muscle system," *Biological Cybernetics*, vol. 102, no. 1, pp. 31–44, 2010.

[23] C. Yang, G. Ganesh, A. Albu-Schaeffer, and E.Burdet, "Human like adaptation of force and impedance in stable and unstable tasks," *IEEE Transactions on Robotics*, vol. 27, no. 5, pp. 918–930, 2011.

[24] C. Yang and E. Burdet, "A model of reference trajectory adaptation for interaction with objects of arbitrary shape and impedance," in *the Proceedings of 2011 IEEE/RSJ International Conference on Intelligent Robots and Systems (IROS)*, (San Francisco, US), pp. 4121–4126, October 18-22 2011.

[25] G. Ganesh, N. Jarrassé, S. Haddadin, A. Albu-Schaeffer, and E. Burdet, "A versatile biomimetic controller for contact tooling and haptic exploration," in *Robotics and Automation (ICRA), 2012 IEEE International Conference on*, pp. 3329–3334, IEEE, 2012.

[26] L. Guo, "Self-convergence of weighted least-squares with applications to stochastic adaptive control," *Automatic Control, IEEE Transactions on*, vol. 41, no. 1, pp. 79–89, 1996.

[27] P. Corke, *Robotics, Vision and Control: Fundamental Algorithms in MATLAB*, vol. 73. Springer, 2011.